



Prediction of Risk Zones and Wildlife Exposure Assessment in Periyar Tiger Reserve using Machine Learning Approach in Kerala, India

Veeramani S, Patil Suyog Subashrao and R.S. Suja Rose¹

Periyar Tiger Conservation Foundation, Periyar Tiger Reserve (East Division), Thekkady, Idukki (DT)-685 509, India

¹Department of Environmental Remote Sensing and Cartography,

School of Earth and Atmospheric Sciences, Madurai Kamaraj University, Madurai-625 021, India

E-mail: Veeramanitkp@gmail.com

Abstract: Forests are extremely risky and these risks frequently cause animals to go extinct. Similar to other hilly regions, the Periyar Tiger Reserve is habitat to a variety of natural hazards and animal-human interactions, although it is unclear how the risk areas are spread or how the exposed species are distributed. The high-resolution trans boundary models illustrating risk to floods, landslides, wildfires, and human-wildlife interactions is proposed in order to assess wildlife distribution vulnerability to high-risk zones across the Periyar Tiger Reserve. An inventory map of the first Using field surveys and various official data, four different types of risks flood, landslides, forest fires, and Human wildlife conflict were created. Using the Max Ent (Maximum Entropy) machine learning technique, a total of 13 geo-environmental parameters were chosen as predictors to create the risk maps. Generating receiver operating characteristic (ROC) curves and computing the area under the ROC curve (AUCROC) allowed us to assess the predictive models' accuracy. The Max Ent model not only performed exceptionally in terms of degree of fitting but also produced significant results in terms of predictive performance. Indicators of the relative relevance of the four categories of risks under study revealed that elevation and distance from streams were, two most crucial determinants for flooding. For detecting landslides, soil, topographic roughness index, and forest cover were important factors. The closest roads, the amount of forest cover, and livestock were each ranked as the three most crucial determinants for human-wildlife conflict. The research area's annual mean temperature, elevation and distance from water bodies, as well as the presence of livestock, were key factors in the mapping of forest fires. An integrated multi-hazard map was finally produced by merging the high-risk zones for flood, landslides, wildfire, and Human wildlife conflict risk. The results demonstrated that 55 % of the area is subjected to risks, reaching a proportion of landslides up to 31%, human wildlife conflict up to 9%, flood up to 5% and fire up to 10 % in the whole territory. Human settlements in the Periyar Tiger Reserve are disproportionately concentrated in areas of high risk. In contrast, low-risk areas are disproportionately unpopulated. Nearly half of Tiger population in the region lives in areas that are highly susceptible to landslide. Few percentages of elephant population live in areas that are highly suspect able to human wildlife conflict zones. Fire and flood risk areas suspect able to the wildlife is comparatively less. Using this type of multi-hazard map may be a useful tool for local administrators to identify areas susceptible to hazards at large scales as we demonstrated in this research.

Keywords: Risk map, Machine Learning algorithms, Periyar Tiger reserve, Wildlife exposure

The IPCC's 6th Assessment Report highlights the profound impact of climate change, particularly in mountain regions, where increased warming and extreme precipitation are expected to lead to cascading consequences such as floods, landslides, and other hazards. Mountainous areas, while providing essential resources to downstream regions, also face significant vulnerability due to their topography, geological processes, and hydrological characteristics (IPCC 2021). Globally, mountain regions account for a majority of hazard-related fatalities, underscoring the urgency of addressing multi-hazard risks in these areas. Agenda 21, established in 1992, emphasizes the importance of sustainable mountain development, stressing the need for risk evaluation and mitigation strategies. With mountain populations growing and urbanizing, the need for effective hazard management is more pressing than ever.

In the Western Ghats, forest fires are a frequent natural disturbance, especially during the summer months. Geospatial techniques have been employed to identify and map fire risk zones in the Periyar Tiger Reserve. Factors such as land cover type, slope, distance from settlements and roads, and elevation were considered in this study. The resulting Fire Risk Index methodology categorizes the area into five risk zones, verified using historical fire incidence data. This risk zone map provides valuable insights for resource managers and planners to implement effective mitigation measures (RS Ajin et al 2015). Similarly, studies in other regions such as Iran and Austria have utilized advanced machine learning techniques to produce multi-hazard risk maps for floods, landslides, wildfires, and other natural events. These maps, derived from comprehensive environmental data and predictive models, offer crucial

information for risk management and disaster mitigation efforts. By integrating hazard susceptibility mapping with land use planning, these studies aim to reduce vulnerability and enhance resilience in hazard-prone areas (Soheila Pouyan et al 2021).

In the Kangchenjunga Landscape, efforts have been made to map human-wildlife conflict hotspots using Max Ent coupled with relevant environmental variables. These hotspots, identified based on factors like road proximity and protected area fragmentation, highlight the need for landscape-level approaches to mitigate conflicts between humans and wildlife. Restoring fragmented habitats and implementing comprehensive conservation strategies are essential steps in addressing human-wildlife conflicts and ensuring the coexistence of both populations (Prashanti Sharma et al 2020). For the Periyar Tiger Reserve in Kerala, there is a crucial need to map risk zones and assess wildlife exposure, particularly concerning landslides, wildfires, floods, and human-wildlife conflict. This research endeavour will provide vital information for policymakers and planners to identify high-risk areas and implement effective mitigation measures, ultimately enhancing the resilience of both ecosystems and communities. The objectives are to identify and prioritize factors influencing flood, forest fire, landslide, and human-wildlife conflict risk zones. Separate maps for each risk zone using the Max Ent algorithm will be created, along with a map of the Tiger Reserve's risk hotspots. Additionally, understanding wildlife distribution, especially mammal exposure to high-risk zones, is a key goal.

MATERIAL AND METHODS

Study area: Periyar Tiger Reserve, located in the Cardamom and Pandalam Hills of the Southern Western Ghats, spans latitudes 9° 17' 56.04" to 9° 37' 10.2" N and longitudes 76° 56' 12.12" to 77° 25' 5.52" E. It falls within Idukki, Kottayam, and Pathanamthitta Districts of Kerala. Established in 1950 as the Periyar Wildlife Sanctuary, it was designated as a Tiger Reserve in 1978, covering 925 km², with 881 km² as core habitat and 44 km² as buffer (Fig. 1). It harbors significant biodiversity, hosting 41% of Kerala's flowering plants, including 26% endemic to the Southern Western Ghats. The reserve supports a variety of flora and fauna, including 17 possibly extinct species and unique plants like *Habenaria periyarensis*. With over 350 medicinal plant species and endangered fauna such as tigers, elephants, and lion-tailed macaques, it is vital for conservation. Periyar is home to 66 mammal species, 342 bird species, and diverse reptiles, amphibians, fishes, and butterflies. It serves as a critical link in maintaining forest connectivity in the Western Ghats. The park experiences an average rainfall of 914mm to 2010mm

and temperatures ranging from 15 to 30 degrees Celsius, with its highest point at 2017 meters above sea level. Vegetation includes evergreen, deciduous, and semi-evergreen forests, as well as grasslands. It is traversed by NH 183, connecting Theni in Tamil Nadu to Kollam in Kerala.

Data and methods: All hazard instances were recorded as points and environmental covariates were continuous or categorical raster layers. Geographic patterns in hazard locations are summarized in Figure 2. Variables used are summarized in Table 1. Periyar Tiger conservation foundation provided data for the years 2001-2021. In this study, however, only 56 spatiotemporally independent fire incidents, 20 flood incidents, 17 conflict locations and 9 landslide locations were used to create the model. After testing the spatiotemporal data using the software package Diva GIS, the auto-correlated sites were eliminated (DIVA GIS version 2). If more than one observation was aggregated in a grid, only one location per 1 km grid cell was used (i.e., to avoid autocorrelation with low sample size).

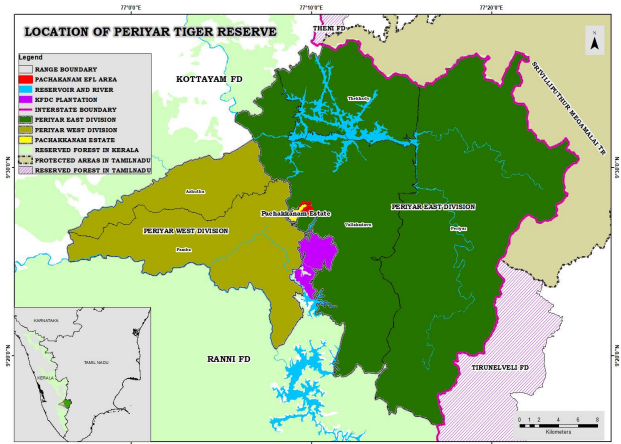


Fig. 1. Location of study area

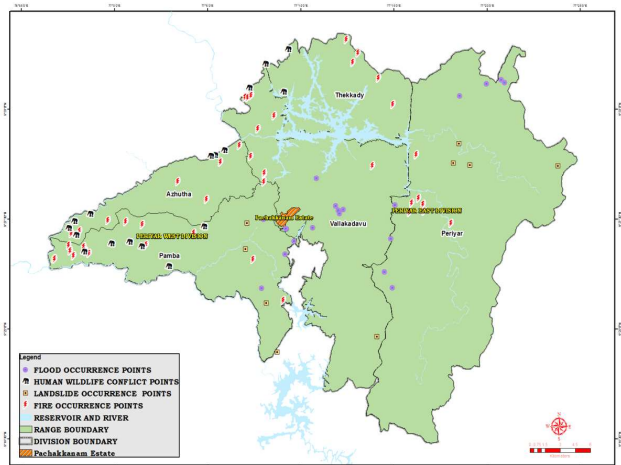


Fig. 2. Hazard locations map (Last 20 years)

Digital elevation model: Topography plays a crucial role in shaping hazard-prone environments, with eleven topographic environmental factors considered: elevation, slope, aspect, terrain wetness index, terrain position index, terrain ruggedness index, stream power index, LS factor, plan curvature, profile curvature, and flow accumulation. These factors influence water movement and soil stability, commonly incorporated into hazard models assessing flood and landslide susceptibility. The digital elevation model (DEM) utilized is from ALOS PALSAR DEM (2014), obtained through radar interferometry with a 12.5m resolution, overcoming cloud cover limitations in the study area. ALOS PALSAR data and its derivatives have been instrumental in hazard assessments for flooding, forest fires, landslides, and human-wildlife conflict in PTR. Slope is determined by the highest magnitude first derivative across each cell of the ALOS PALSAR DEM, while aspect denotes the down slope direction. Flow accumulation measures the number of cells upslope from any given cell, crucial for understanding water movement through watersheds. Topographic wetness index quantifies terrain-driven variation in soil moisture, aiding in hazard prediction. Topographic position index helps distinguish topographic features, while terrain ruggedness index expresses elevation differences between adjacent cells. Stream power index estimates the erosive power of flowing water, predicting potential gully formation. The LS-factor combines slope length and steepness, reflecting soil loss. Profile curvature indicates the direction of maximum slope, affecting flow acceleration or deceleration, while plan curvature reflects the curvature of contours, influencing water flow direction. These variables were derived using ArcGIS 10.3.

Normalized differential vegetation index: The normalized difference vegetation index (NDVI), which is derived from remote-sensing (satellite) data, is closely linked to drought conditions. To determine the density of green on a patch of land, the distinct colours (wavelengths) of visible and near-infrared sunlight reflected by the plants are observed. Range of NDVI is -1 to $+1$. Higher value of NDVI refers to healthy and dense vegetation. Lower NDVI values show sparse vegetation. The Normalized Difference Vegetation Index is prepared by using Sentinel-2 images where band 8 is Near Infrared and band 4 is Red. The NDVI can be calculated from,

$$NDVI = \frac{(BAND8 - BAND4)}{(BAND8 + BAND4)}$$

Forest cover: Forest cover is a significant factor in forming hazard-prone environments and is often integrated into susceptibility models (Rimal et al 2015, Aryal et al 2020, Vilà-Villardell et al 2020). In the PTR, forest cover is classified into categories such as moist deciduous forest, evergreen and semi-evergreen forest, thickets, grassland, and water bodies. Classification was conducted using a supervised algorithm on Sentinel-2 imagery, with 70% of the ground truth dataset used for classification and 30% for testing. The overall accuracy of the classification process was determined to be 95.57% (Veeramani et al 2023).

Lithology and fault: The dominant rock types in the Mullaperiyar region, forming the core and buffer areas of the PTR, are Precambrian crystalline rocks, primarily the Charnockite-Khondalite-migmatite complex. Charnockite is prevalent, with hornblende gneiss in the eastern side. The gneissosity trend varies from WNW-ESE to NE-SW, exhibiting symmetrical and asymmetrical antiforms and

Table 1. Predictor variables tested for prediction modelling of various Risk in PTR

Data description	Type	Source	Derived Layers
Sentinel-2-10 m	Raster	USGS Earth Explorer	NDVI
ALOS PALSAR-DEM-12.5 m	Raster	Alaska Satellite Facility-Vertax	Elevation, Slope, Aspect, Accumulation, TRI, Plan curvature, Profile Curvature, TPI, TWI, SPI, LS factor
Annual Temperature	Raster	Periyar tiger conservation foundation	
Annual Precipitation	Raster	Periyar tiger conservation foundation	
Forest Cover	Raster	FSI-2019	Sentinel-2
Soil Suborder	Raster	FAO-UNESCO,2005	
Lithology	Raster	GSI, India	
Water body	Raster	SOI TOPOSHEET	Distance from Water Source
Settlements	Raster	SOI TOPOSHEET	Distance from Settlements,
Linear networks	Raster	SOI TOPOSHEET	Distance from Roads, Trekpath, Power lines
Faults	Raster	SOI TOPOSHEET	Distance from faults
Streams	Raster	SOI TOPOSHEET	Distance from Streams
Livestock	Raster	https://livestock.geo-wiki.org/home-2/	1*1 km Grid

synforms, with an observed overturned and refolded antiformal structure in the central area, passing through Mullaperiyar. Major crustal discontinuities include the NW-SE trending Muvattupuzha fault, WNW-ESE trending Achankovil shear zone, and NNW-SSE striking Udumbanchola fault. Visible lineaments around the reservoir contribute to the shape of Periyar Lake, reflecting topographic lows and valleys. The lake's EW shape with arms oriented towards NNW, NE, and north correlates with these lineaments. The area exhibits a higher lineament density compared to adjacent parts, indicating significant past tectonic activity, with the Udumbanchola and Cumbam faults intersecting in the reservoir area.

Soil: The properties of a soil affect its contribution to hazard-forming environments. For example, the shear strength of a soil is a property related to its propensity to slide, and a soil suborder's permeability affects how water moves through its matrix of or over its surface. In these models, FAO-UNESCO world soil suborder data were included as a categorical covariate at a resolution of 0.033 decimal degrees. This soil map is not remotely sensed, but is based on ground surveys and national data. Soil moisture is related to the incidence of landslides and floods. High soil moisture lowers the shear strength of a soil, preconditioning slope failure and land sliding, and increases surface runoff, in turn increasing peak flow and flooding (Wasko and Nathan 2019). Soil moisture data for the study region at a 15-km resolution was obtained from those published by the European Space Agency's Climate Change Initiative. These data represent the average annual soil moisture values in volumetric water content (m³/m³) from 1991 to 2016.

Distance to settlement: The 44 sq.kms of forest types in Buffer zone encompasses Human settlement, leased area, office buildings and other supporting facilities for tourism and education and awareness. There are 3 tribal settlements in the buffer zone of PTR (East). Apart from these settlements there are no other settlement inside PTR, East Division. Five EDC-Eco Development Committee are operating in these three tribal settlements (Table 2).

Distance to waterbody: Fluvial flooding occurs when a water body exceeds its capacity and floods its adjacent area, and thus has a direct relationship with the distance from a water body. Each cell in the study region was assigned a value describing its distance in decimal degrees to the nearest permanent water cell. Permanent water was defined as water that occurred more than 85% of the time. These data were derived from the Global Surface Water Explorer, a dataset that quantifies global surface water changes between 1984 and 2015 at 30-meter resolution (Pekel et al 2016). These data are commonly cited in models of hydrologic hazards in the PTR

(Mohanty and Maiti 2021, Veh et al 2019).

Distance to streams: Many streams feeding the two major rivers viz. Periyar and Pamba are perennial. Unlike the streams in the evergreens above 1000m, some of the streams feeding Pamba and Azhutha dry up in peak summer. Except for a few, the marshes and streams on the grassy hill tops around the lake also dry up. The water level in lake fluctuates between a maximum of 41.5m (136 feet at the full reservoir level) to a minimum of 32m (104.9869 feet). A number of bunds, check dams and artificial pools have been made over the years, which hold water even during peak summer. Water sources along the traditional pilgrim routes are used by a large number of pilgrims during the pilgrimage season. The water of Pamba below Sabarimala becomes severely polluted due to human waste by the end of the pilgrim season in January. People as well as livestock utilize some of the water sources near Thekkady. The canal leading from the reservoir to the pen-stoke is put to variety of uses like bathing, washing etc. The check dam prevents the effluents from Kumily town from seeping into the reservoir. However, during heavy rains the check dam overflows into the canal. Part of the reservoir in buffer is utilized for providing boating facilities for tourists. Since the India Eco-development Project, fishing by tribes is regulated. In addition, the lake meets the water needs of people of Kumily.

Distance to Road: There are two major roads present inside the park which is given below

- Kozhikanam - Aruvioda and Zero - Pachakkad roads and culverts are to be maintained.
- The existing Meenar coupe road is to be maintained and culverts reconstructed in order to patrol even during monsoon season.

Distance to power line: There are 4 high tension power line passing through Periyar East Division. Details of power line is given in (Table 3). There is always a risk of fire occurrence from these transmission lines.

Precipitation and temperature: The Tiger Reserve experiences two distinct monsoon seasons with highly variable rainfall patterns across the area. Maximum recorded rainfall reached 5803 mm at Pachakanam in 2007, while the lowest was 1145 mm at Thannikudy in 2010. About two-thirds of the total rainfall occurs during the southwest monsoon from June to September, while the northeast monsoon

Table 2. Settlements within PTR east division

Settlements	Community	No. of families	No. of members
Labbakandam (Mannakudy)	Mannan tribe	327	1268
Labbakandam (Paliyakudy)	Paliyan tribe	153	453
Vanchivayal	Urali tribe	74	264

typically lasts from October to December, influencing management strategies. July is the wettest month, with January being the driest. December to April is generally considered the dry season, with temperatures ranging from 11°C to 27°C. The hottest months are April and May, while December and January are the coolest. Lowest humidity is observed from February to April. Dew formation in December-January keeps vegetation green, particularly grass. The South-West monsoon brings maximum wind velocity. The reserve has two major rivers with perennial feeder streams and reservoirs, ensuring water availability year-round. Severe drought, experienced in 1983, led to extensive forest fires. Some streams feeding the major rivers may dry up in peak summer, along with marshes and streams around the lake, although water levels are regulated between 41.5 m and 32 m through bunds, check dams, and artificial pools, ensuring water retention even in peak summer.

Environmental covariate data resampling: Raster grids for all environmental data were resampled to 16 arcsecond (approximately 0.5 km) resolution. Continuous covariates were resampled using bilinear interpolation. Soil suborder was up sampled by assigning the value of the original larger cell to each new smaller cell within its bounds. Land cover was down sampled by assigning each new cell the most common value of the original cells within its bounds.

Wildlife distribution data: The distribution of tigers and elephant is collected using the 8-day protocol exercise and also during regular perambulation by frontline staff. Status of distribution of the carnivores is also being analyzed annually based on the sign survey carried out by the staff during patrolling. In addition, data on encounter rate is also being collected as part of *All India Tiger Monitoring Program and camera trapping exercise*. The data collected from survey blocks ranging in size from 10 to 25 km² as part of 'Monitoring of Tigers, Co-predators, Prey and their Habitat' was used to assess the presence absence of tiger and co-predators. The total of 59 such blocks were used for collecting the

information and the data collected was analyzed to find out the density distribution of tigers and elephants. And these data were used to find the wildlife exposure in High-risk zones.

Modelling: The Max Ent software (version 3.3.3.e; <http://www.cs.princeton.edu/schapiro/maxent/>) was utilized for fire modelling, generating probability distribution maps based on similar situations across terrain using maximum entropy techniques and considering GPS coordinates (Elith et al 2011). Even with limited presence records, Maxent predicts species' ecological niches effectively. This study aimed to develop a fire prediction model based on Max Ent's principles, which minimize relative entropy between presence-only instances and background landscape data. Unlike traditional approaches like logistic regression or random forest, Max Ent utilizes presence-background data to predict forest fires, reducing assumptions and sample selection bias risks. Recent software versions incorporate transformation methods to standardize features and prevent overfitting. Max Ent is particularly suitable for forest fire investigations due to its reliance on presence-only data (Arnold et al 2014, Phillips and Elith 2013).

Parameter settings: Initially, all feature maps were projected from the GCS-WGS-1984 geographic projection system to the WGS-1984-UTM-Zone-43 N plane projection system, which is adequate for the research area. The polyline vector maps of the power line, water bodies network, and point vector map of human habitations were then used to create Euclidean distance raster maps. These raster maps were created to determine the distance between seismic occurrences and power lines, water bodies, and human settlements. The DEM was used to create topographic feature maps of Elevation, Slope, Aspect, Accumulation, TRI, Plan curvature, Profile Curvature, TPI, TWI, SPI, LS factor. This work employed raster maps of averaged NDVI and forest cover to train the algorithm.

Following that, all feature maps were re sampled to the

Table 3. Power lines in PTR

Division	Range	Section	Name of the power line project	Length (km) approx.	Width (m)	Area (sq.km)
PTR-East	Thekkady	Edapalayam	Moozhiyar-Theni- 110 KV	5.2	15	0.078
PTR-East	Vallakkadavu	Thondiyar	Thondiyar - Manamuttymala 220 KV	6	25	0.15
PTR-East	Vallakkadavu	Vallakkadavu	Moozhiyar - Vandiperiyar - 110 KV	9.2	30	0.276
PTR-East	Vallakkadavu	Vallakkadavu And kozhikanam, Kalaradichan	Vallakkadavu-Pachakanam Estate-11 KV	8	25	0.2

same spatial extent and 10 metre cell size as the NDVI raster. Following that, the feature maps were normalized so that their pixel values were in the range of 0 to 1 (Chang 2017). This is a standard machine learning approach for reducing calculation time. All of these geo processing techniques were carried out in the Arc GIS environment. Because the normalized maps are easily readable by Max Ent, they were exported in ASCII format. Comma-Separated Values (CSV) file was also created from the presence-only dataset of forest hazard events. Max Ent is a java program-based package that was employed in this investigation. All of the feature maps were stacked with matching extents during the creation of the prediction map, and feature attributes were retrieved from the feature stack using the presence-only datasets re event coordinates. The presence-only dataset was thus data trimmed, resulting in a more credible dataset. The dataset was split into two parts: 25% was utilized for testing, while the rest was used to train Max Ent. For cross validation, the training dataset was also partitioned into ve-folds. Following that, a background dataset was created by picking 1000 random points from the research area's perimeter. There is a maximum of 5,000 backdrop points, and linear, quadratic, and hinge features were utilized (Phillips and Dudik 2008). For model creation (Flory et al 2012), 100 repetitions were preserved, and the occurrence sites were randomly partitioned into two sub samples, with 75 percent of the locations used as the training dataset and the remaining 25% used to test the resulting (partitioned) models. The model's accuracy was measured using the area under the curve (AUC) of a receiver operating characteristic (ROC) plot (ranging from 0.5 = random to 1 = perfect discrimination). The Jack knife method was used to determine the factors' importance (Yang et al 2013). A probability map of various risks was created using an average of 100 model projections. The model parameters and values, on the other hand, were left at their default levels. Additionally, all values between 0.6 and 0.8 as high-risk zones, and those between 0.2 and 0.6 as Medium Risk zones, values below 0.2 were determined as low risk zones.

RESULTS AND DISCUSSION

Forest fire risk mapping: Fifty six fire incidences were found to be Spatio-temporally independent. Jack knife test results showed that based on the percentage contribution, "Distance to settlement " (17 %), "Temperature" (temp) (16.7%), "distance to water body" (d2w) (16.3 %) and "Forest cover" (10.6%) were the highest contributors. Based on permutation importance, "Precipitation of seasonality" (bio15) was the most significant variable (16.6%) followed by "Temperature" (temp) (29.8%) (Table 4). The area under the

curve (AUC) score was 0.955 for the training data from our model, which indicates moderate to excellent predictive ability of the model (Fig. 5). The classified fire prediction map showed good discrimination between high, medium and low fire risk categories. The result demonstrated that out of the total geographical area of Periyar tiger reserve 96 sq.km area (10.3%) was under high-risk category, 1.5 ha area (0.001%) under medium risk and 803 sq.km area (86.8%) under low-risk category (Fig. 6). The areas near to village having moderate canopy density were highly affected by fire.

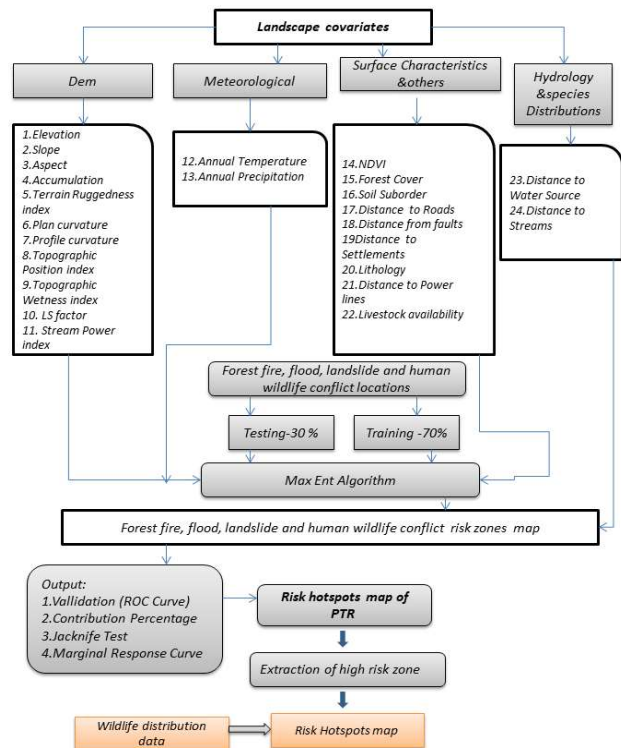


Fig. 4. Methodology

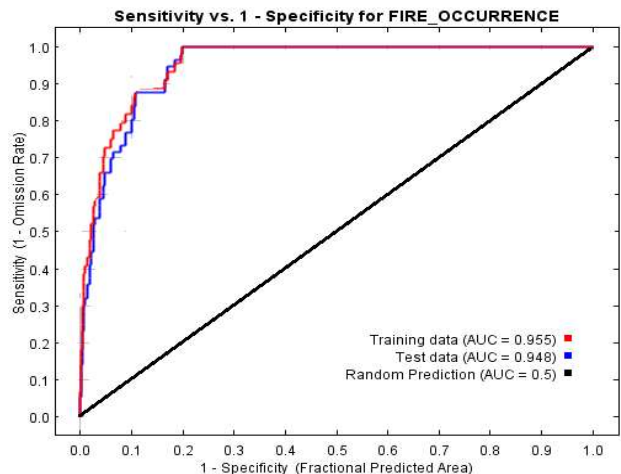


Fig. 5. Area under curve of fire (AUC)

Flood risk zone mapping: Twenty flood incidences were spatio-temporally independent. Jack knife test results showed that based on the percentage contribution, "Distance to stream " (32.8 %), "Temperature" (temp) (24 %), "Digital Elevation model" (Dem) (10.3 %) and "Rainfall" (9.3 %) were the highest contributors. Based on permutation importance, "distance to stream" (stream) was the most significant variable (37.6 %) followed by "Temperature" (temp) (14 %) (Table 5). The area under the curve (AUC) score was 0.979 for the training data from our model, which indicates moderate to excellent predictive ability of the model (Fig. 7).

Landslide risk zone mapping: Nine landslide incidences were found to be spatio-temporally independent. Jack knife test results showed that based on the percentage contribution, "soil " (51.5 %), "topographic roughness index " (tri) (28.8 %), "Forest cover" (fc) (12.2 %) and "NDVI (4.9 %) were the highest contributors. Based on permutation importance, "soil" (stream) was the most significant variable (39.7 %) followed by "Topographic roughness index" (tri) (31.1 %) (Table 6). The area under the curve (AUC) score

was 0.923 for the training data from our model, which indicates moderate to excellent predictive ability of the model (Fig. 9). The classified flood prediction map showed good discrimination between high, medium and low flood risk categories. The result demonstrated that out of the total geographical area of Periyar tiger reserve 48 sq.km area (5.1%) was under high-risk category, 148 sq.km area (16 %) under medium risk and 703 sq.km area (76 %) under low-risk category (Fig. 8). The areas near to waterfalls were highly affected by flood. The classified landslide prediction map showed good discrimination between high, medium and low flood risk categories. The result demonstrated that out of the total geographical area of Periyar tiger reserve 290 sq.km area (31 %) was under high-risk category, 388.75 sq.km area (42%) under medium risk and 220 sq.km area (23 %) under low-risk category (Fig. 10). The areas near to streams having were highly affected by landslide.

Human wildlife conflict zone mapping: Seventeen conflict incidences were found to be spatio-temporally independent. Jackknife test results showed that based on the percentage

Table 4. Percent contribution and permutation importance of variables (Fire)

Variable	Code	Percent contribution (%)	Permutation importance (%)
Live stock availability	livestock	17	7.4
Temperature	temp	16.7	29.8
Distance to waterbody	d2w	16.3	6
Forest cover	fc	10.6	0.4
Distance to road	ro	9.7	0
Rainfall	rainfall	7.1	12.2
Soil Suborder	soil	5.7	2.5
Digital elevation model	dem	3.9	23.3
Normalized difference vegetation index	ndvi	3	4.6
Distance to powerline	power	2	4.9
Flow accumulation	fa	1.9	2.2
Aspect	asp	1.6	3.1
Lithology	litho	1.3	0
Distance to streams	stream	0.7	0.4
Distance to faults	fault	0.7	0.7
Terrain ruggedness index	tri	0.6	1.9
Topographic position index	tpi	0.4	0.1
Stream power index	spi	0.2	0
Plan curvature	plan	0.2	0.3
Slope	slope	0.2	0
Profile curvature	profile	0.1	0.1
Distance to Settlements	ts	0.1	0.2
LS Factor	lsfactor	0	0
Topographic wetness index	twi	0	0

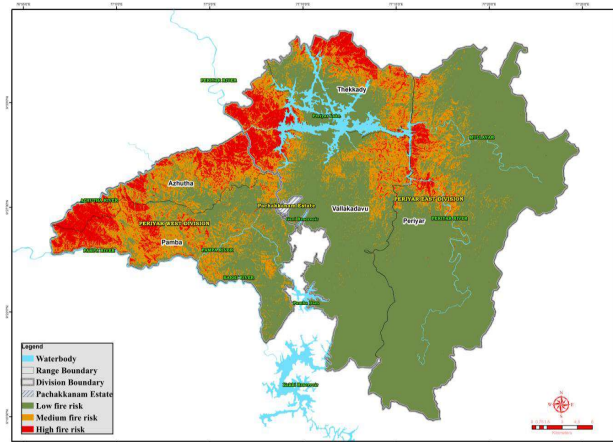


Fig. 6. Classified fire risk map

contribution, "distance from road" (ro) (30.1 %), "Livestock" (19.3 %), "Forest cover" (fc) (17.3 %) and "Distance to waterbody" (d2w) (7.7 %) were the highest contributors. Based on permutation importance, "distance to road" (ro) was the most significant variable (42.5 %) followed by "livestock" (21.4 %) (Table 7). The area under the curve (AUC) score was 0.986 for the training data from our model, which indicates moderate to excellent predictive ability of the

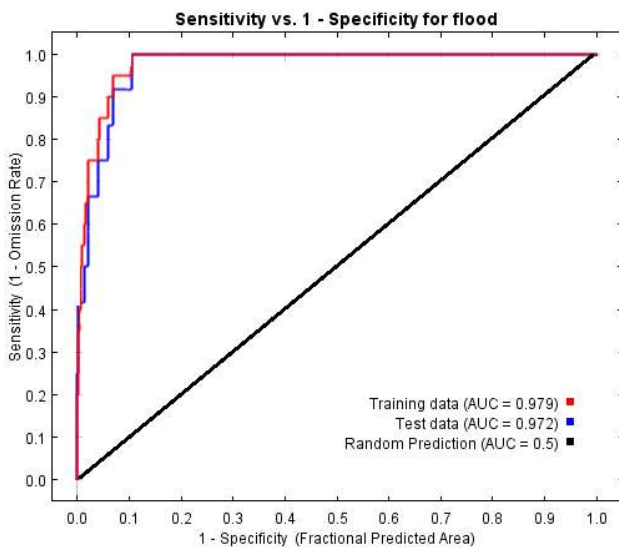


Fig. 7. Area under Curve of Flood (AUC)

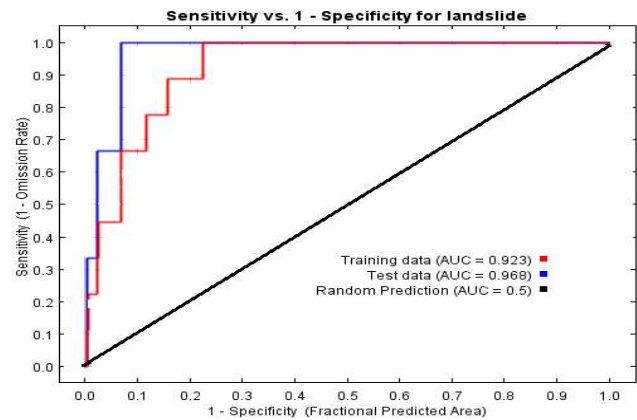


Fig. 9. Area under Curve of landslide (AUC)

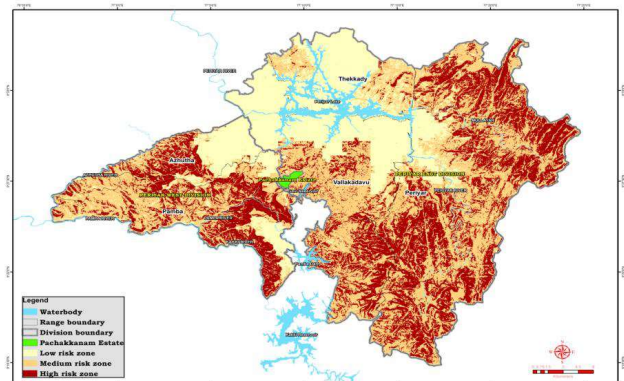


Fig. 10. Classified landslide risk map

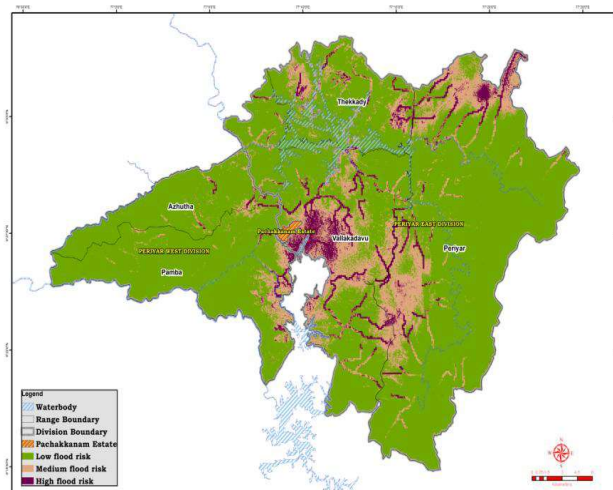


Fig. 8. Classified flood risk map

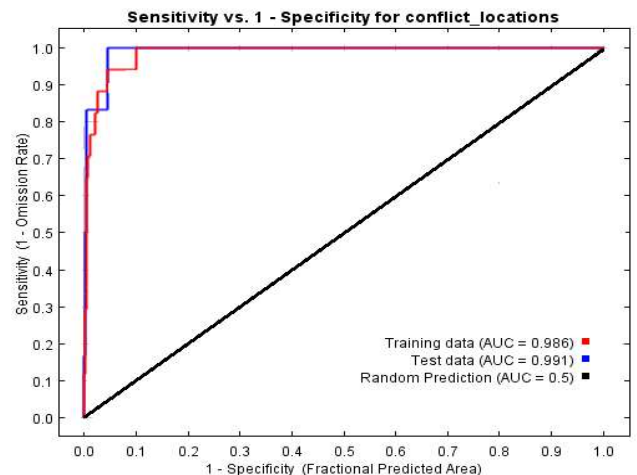


Fig. 11. Area under Curve of HWC (AUC)

model (Fig. 11). The classified human wildlife conflict prediction map showed good discrimination between high, medium and low human wildlife conflict risk categories. The result demonstrated that out of the total geographical area of Periyar tiger reserve 81 sq.km area (8.7 %) was under high-risk category, 103.51 sq.km area (11.11%) under medium risk and 714 sq.km area (77 %) under low-risk category (Fig.

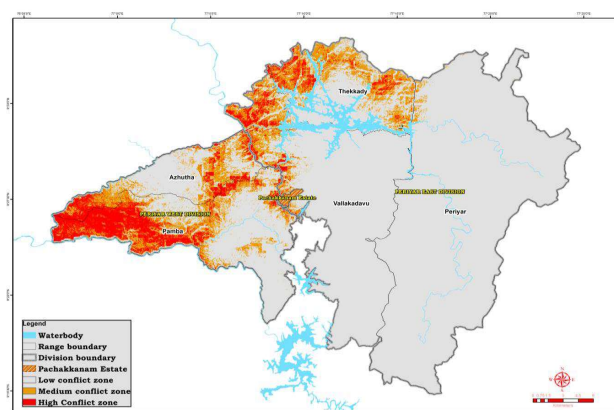


Fig. 12. Classified human wildlife conflict risk zone map

12). The areas near to fringe villages having moderate canopy density were highly affected by human wildlife conflict.

Risk hotspots map prepared using high risk zones of forest fire, flood, landslide and human wildlife conflict. It demonstrated that 55 % of the area is subjected to risks (Fig. 13), reaching a proportion of landslides up to 31%, human

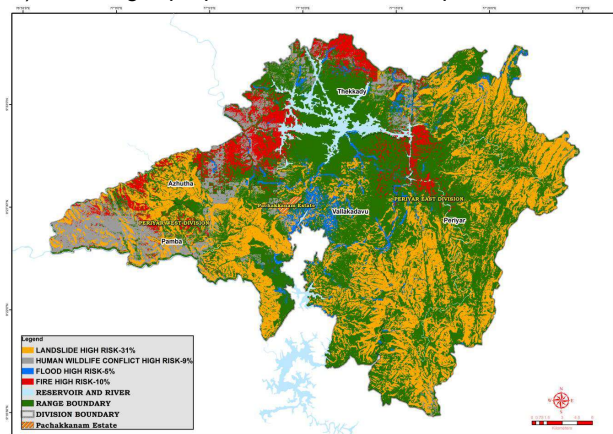


Fig. 13. Risk hotspot map of Periyar Tiger Reserve

Table 5. Percent contribution and permutation importance of variables (Flood)

Variable	Code	Percent contribution (%)	Permutation importance (%)
Distance to streams	stream	32.8	37.6
Temperature	temp	24	14
Digital elevation model	dem	10.3	23.6
Rainfall	rainfall	9.3	8.5
Live stock availability	livestock	7.1	3.4
Distance to faults	fault	5.2	6.1
Distance to waterbody	d2w	3	0
Forest cover	fc	2	1.5
Soil suborder	soil	1.5	0
LS factor	lsfactor	1	2.2
Normalized difference vegetation index	ndvi	0.9	1.2
Topographic wetness index	twi	0.8	0.1
Aspect	asp	0.8	1
Distance to road	ro	0.5	0.6
Plan curvature	plan	0.3	0
Slope	slope	0.3	0
Distance to settlements	ts	0.1	0.1
Flow accumulation	fa	0	0.1
Terrain ruggedness index	tri	0	0
Profile curvature	profile	0	0
Lithology	litho	0	0
Stream power index	spi	0	0
Topographic position index	tpi	0	0
Distance to powerline	power	0	0

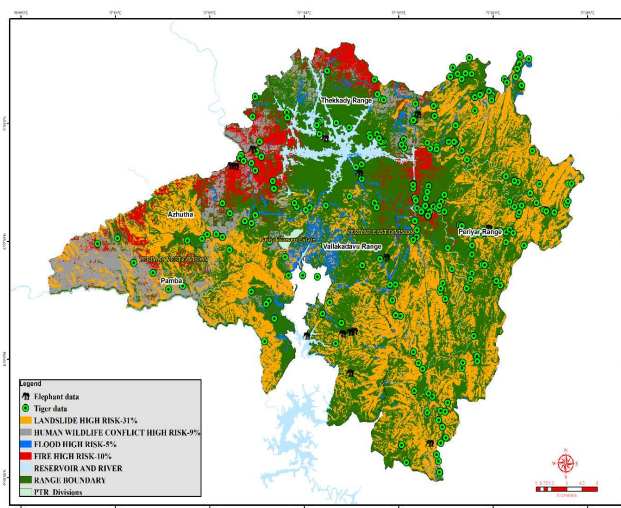


Fig. 14. Wildlife risk exposure map

Table 7. Percent contribution and permutation importance of variables (HWC)

Variable	Code	Percent contribution (%)	Permutation importance (%)
Distance to road	ro	30.1	42.5
Live stock availability	livestock	19.3	21.4
Forest cover	fc	17.3	1.3
Distance to waterbody	d2w	7.7	0.1
Soil suborder	soil	6.2	7.9
Distance to settlements	ts	4	0.1
Distance to streams	stream	3.1	18.8
Normalized difference vegetation index	ndvi	2.6	1.1
Distance to powerline	power	2.4	0
Lithology	litho	1.8	0
Aspect	asp	1.5	0.4
Plan curvature	plan	1.2	1.6
Flow accumulation	fa	1.1	2
Slope	slope	0.9	0
Terrain ruggedness index	tri	0.4	0.2
Distance to faults	fault	0.3	1.5
Temperature	temp	0.1	0.8
Digital elevation model	dem	0	0
LS factor	lsfactor	0	0.3
Profile curvature	profile	0	0.1
Rainfall	rainfall	0	0
Stream power index	spi	0	0
Topographic position index	tpi	0	0
Topographic wetness index	twi	0	0

Table 6. Percent contribution and permutation importance of variables (Landslide)

Variable	Code	Percent contribution (%)	Permutation importance (%)
Soil suborder	soil	51.5	39.7
Terrain ruggedness index	tri	28.8	31.1
Forest cover	fc	12.2	1.5
Normalized difference vegetation index	ndvi	4.9	6.3
Distance to streams	stream	1.9	19.4
Stream power index	spi	0.5	2
Flow accumulation	fa	0.1	0
LS Factor	lsfactor	0	0
Distance to powerline	power	0	0
Plan curvature	plan	0	0
Live stock availability	livestock	0	0
Lithology	litho	0	0
Distance to faults	fault	0	0
Topographic wetness index	twi	0	0
Distance to settlements	ts	0	0
Topographic position index	tpi	0	0
Temperature	temp	0	0
Slope	slope	0	0
Distance to road	ro	0	0
Rainfall	rainfall	0	0
Profile curvature	profile	0	0
Digital elevation model	dem	0	0
Distance to waterbody	d2w	0	0
Aspect	asp	0	0

wildlife conflict up to 9%, flood up to 5% and fire up to 10 % in the whole territory.

Exposure of wildlife population: The human settlements in the Periyar Tiger Reserve are disproportionately concentrated in areas of high risk. In contrast, low-risk areas are disproportionately unpopulated. Nearly half of Tiger population in the region lives in areas that are highly susceptible to landslide. Few percentages of elephant population live in areas that are highly susceptible to Human wildlife Conflict zones. Fire and flood risk areas susceptible to the wildlife is comparatively less. This area comprises only 55 % of the study region, but is home to 50% of its population (Fig. 14).

CONCLUSIONS

Analyzing climate change-related risk events is crucial for protecting forests from further degradation in India. Research

is urgently needed in risk detection, suppression, and risk ecology to better manage forest risks. This study evaluates long-term forest fire, flood, landslide, and human-wildlife conflict events across India's state boundaries, seasonal trends, land use and land cover categories, and future climate anomalies. The methodology used here is more advanced than previous frequency analysis methods, offering improved accuracy in risk prediction. GIS-based modelling helps identify, map, and quantify biophysical characteristics and predict future risks. The developed risk model is vital for identifying and controlling risks in Western Ghats protected areas, aiming to reduce hazard events and losses. The 55% of the area is at risk, with landslides affecting 31%, human-wildlife conflict 9%, flood 5%, and fire 10%. Human settlements in the Periyar Tiger Reserve are concentrated in high-risk areas, while low-risk areas are less populated. The significant portion of the tiger population resides in landslide-prone areas, while a smaller percentage of the elephant population faces high human-wildlife conflict risk. This multi-hazard map can assist local administrators in identifying large-scale hazard-prone areas effectively.

ACKNOWLEDGEMENT

The authors would like to express their gratitude to Field Director (Project Tiger), Periyar Tiger Reserve for their encouragement. The authors additionally thank the Assistant Field Director, Periyar Tiger Reserve for their recommendations and assistance during the investigation. The authors acknowledge the usage of open-source sentinel-2 Data Products.

REFERENCES

- Ajin, RS, Ana-Maria Loghin, Vinod PG and Mathew K Jacob 2016. RS and GIS based forest fire risk zone mapping in the Periyar Tiger Reserve, Kerala, India. *Journal Wetlands Biodiversity* **6**:139-148.
- Bhagawat Rimal, Himlal Baral, Nigel Stork and Kiran Paudyal 2015. Growing city and rapid land use transition: Assessing multiple hazards and risks in the Pokhara Valley, Nepal. *Land* **4**: 957-978.
- Chang KT 2017. *Introduction to Geographic Information Systems* (4 edition). McGraw Hill Education.
- Conrad Wasko and Rory Nathan 2019. Influence of changes in rainfall and soil moisture on trends in flooding. *Journal of Hydrology* **575**: 5895.
- Dibit Aryal, Lei Wang, Tirtha Raj Adhikari and Jing Zhou 2020. A Model-Based Flood Hazard Mapping on the Southern Slope of Himalaya. *Water* **12**: 540.
- Elith J, Phillips SJ, Hastie T, Dudik M, Chee YE and Yates CJ 2011. A Statistical Explanation of MaxEnt for Ecologists. *Diversity and Distributions* **17**: 43-57.
- Georg Veh, Oliver Korup, Sebastian von Specht and Sigrid Roessner 2019. Unchanged frequency of moraine-dammed glacial lake outburst floods in the Himalaya. *Nature Climate Change* **2000**: 1-5
- IPCC 2021. *Summary for Policymakers. In: Climate Change 2021: The Physical Science Basis*. Contribution of Working Group I to the Sixth Assessment Report of the Intergovernmental Panel on Climate Change [Masson-Delmotte, V., P. Zhai, A. Pirani, S.L. Connors, C. Péan, S. Berger, N. Caud, Y. Chen, L. Goldfarb, M.I. Gomis, M. Huang, K. Leitzell, E. Lonnoy, J.B.R. Matthews, T.K. Maycock, T. Waterfield, O. Yelekçi, R. Yu, and B. Zhou (eds.)]. Cambridge University Press, Cambridge, United Kingdom and New York, NY, USA, pp. 3-32.
- James D. Arnold, Simon Brewer and Philip E. Dennison 2014. Modeling climate-fire connections within the great Basin and upper Colorado River Basin, Western United States. *Fire Ecology* **10**: 64-75.
- Lena Vilà Vilardell, William Scott Keeton, Dominik Thom and Choki Gyeltshen 2020. Climate change effects on wildfire hazards in the wildland-urban-interface - blue pine forests of Bhutan. *Forest Ecology and Management* **461**: 117927
- Litan Mohanty and Sabyasachi Maiti 2020. Regional morphodynamics of supraglacial lakes in the Everest Himalaya. *Science of The Total Environment* **751**(11): 141586.
- Phillips SJ and Elith J 2013. On estimating probability of presence from use-availability or presence-background data. *Ecology* **94**: 1409-1419.
- Prashanti Sharma, Nakul Chettri, Kabir Uddin, Kesang Wangchuk, Rajesh Joshi, Tandin, Aseesh Pandey, Kailash Gaira, Khadga Basnet, Sonam Wangdi, Tashi Dorji, Namgay Wangchuk, Vishwas Chitale, Yadav Uprety and Eklabya Sharma 2020. Mapping human-wildlife conflict hotspots in a transboundary landscape, Eastern Himalaya. *Global Ecology and Conservation* **24**: 1284.
- Soheila - Pouya, Hamid Reza Pourghasemi, Mojgan Bordbar and Soroor Rahmanian 2021. A multi-hazard map-based flooding, gully erosion, forest fires, and earthquakes in Iran. *Scientific Reports* **11**(1): 14889.
- Steven J Phillips and Miroslav Dudík 2008. Modeling of species distributions with MAXENT: New extensions and a comprehensive evaluation. *Ecography* **31**: 161-175.
- Veeramani S, Anoop V, Ramesh Babu M, Patil Suyog Subashrao and Suhyb PJ 2023. Forest cover change detection using geospatial techniques in Periyar Tiger Reserve, Kerala, India. *Ecology, Environment and Conservation* **29**: 216-S224
- Xueqing Yang, Satya PS Kushwaha, Jianchu Xu and Sameer Saran 2013. Maxent modeling for predicting the potential distribution of medicinal plant, *Justicia adhatoda* L. in Lesser Himalayan foothills. *Ecological Engineering* **51**: 83-87.